Liquefaction Potential of Railway Embankments

Miguel A. Pando
Virginia Polytechnic Institute and State University, Blacksburg, VA

C. Guney Olgun
Missouri University of Science and Technology, olgun@mst.edu

James R. Martin II
Virginia Polytechnic Institute and State University, Blacksburg, VA

LIQUEFACTION POTENTIAL OF RAILWAY EMBANKMENTS

Miguel A. Pando
Department of Civil and Env. Eng.
Virginia Tech
Blacksburg, Virginia-USA-24061

C. Guney Olgun
Department of Civil and Env. Eng.
Virginia Tech
Blacksburg,.Virginia-USA-24061

James R. Martin, II
Department of Civil and Env. Eng.
Virginia Tech
Blacksburg, Virginia-USA-24061

ABSTRACT

This paper presents an overview of the nature of train-induced vibrations and discusses the liquefaction potential of railway embankments under such low-level vibrations. The paper also presents the results of static and dynamic finite difference numerical analyses performed for a simple railway embankment geometry. The liquefaction potential for the railway embankment foundation was estimated using the results from FLAC numerical analyses, as well as a cyclic shear stress liquefaction resistance approach using a modified cyclic resistance ratio curve. Liquefaction of railway embankment foundations was found to be possible. However, based on the majority of reported failures the liquefaction potential remains low unless the train-induced vibrations are coupled with factors such as loose foundation, and sudden rise of pore water pressures due to poor drainage, flooding, or heavy rainfall.

INTRODUCTION

Failure of railway embankments due to train-induced ground vibrations is not a common occurrence. Nevertheless, several cases have been reported in the literature (e.g. Szerdy, 1985; Carter and Seed, 1988). In most of these cases, the embankment failures have involved loose, saturated cohesionless soils considered to be susceptible to liquefaction. A list of some of the case histories reported in the literature is given in Table 1. The majority of reported failures have been associated with a special combination of factors in addition to train induced vibrations. These may be rises of pore water pressures due to poor drainage, flooding, etc.

This paper provides a brief overview and summary of the available information on the subject of train induced vibrations and investigates the likelihood of liquefaction triggering by these low-level vibrations. Two dimensional static and dynamic analyses were carried out for a typical railway embankment subjected to average train loading to help assess the liquefaction potential of railway embankments.

TRAIN-INDUCED VIBRATIONS

Moving loads, such as trains, have long been recognized as a source of ground vibration (Kaynia et al. 2000). The specific problem of train-induced vibrations has been studied for quite some time (e.g. Griffin and Stanworth, 1984; Carter and Seed, 1988; Zackrisson, 1997; Madshus et al. 1999; Kaynia et al. 2000).

The level of train-induced ground vibrations is a function of several factors such as axle weight, suspension design, train speed, ground conditions and track characteristics such as longitudinal profile and rail joints (Griffin and Stanworth, 1984). Various modeling approaches have been proposed to estimate the level of train-induced vibrations. Detailed descriptions of such approaches can be found in Carter and Seed (1988), Madshus et al. (1999) and Kaynia et al. (2000).

Table 1. Some case histories of railway embankment failures

Date	Location	Description	Reference
1953	Guntorp, Sweden	Railway embankment on sensitive clay with sand seams	Szerdy, 1985
March 6, 1978	Cajon Pass, California	Uncompacted clean sand	Szerdy, 1985; Carter and Seed, 1988
---	San Joaquin River Delta, CA	Sand embankment saturated at base	Carter and Seed, 1988
Sept, 1980	San Francisco Bay area, CA	Sand embankment saturated by flood	Szerdy, 1985
July, 1987	Michigan Highway 94, MI	Sandy roadway embankment during seismic exploration	Hryciw et al. 1990

Several experimental studies in the literature report field observations of ground vibrations recordings (e.g. Barneich, 1985; Kim and Lee, 1998; Carter and Seed, 1998). Measured train-induced ground vibrations have been reported to have frequencies ranging between 10 to 60 Hz (Griffin and Stanworth, 1985; Barneich, 1985; Carter and Seed, 1998). In comparison, earthquake-induced vibrations typically have predominant frequencies ranging from 0.5 to 4 Hz (Seed and Idriss, 1982). The higher frequencies associated with train-induced vibrations are an important difference to consider in a detailed liquefaction analyses.

Train ground motion recordings typically show about 5 seconds of strong shaking followed by about 20 seconds of lower intensity shaking (Carter and Seed, 1988). Carter and Seed measured train-induced peak ground surface accelerations (PGA) of 0.3 g and 0.1 g at 10 ft and 20 feet away from the tracks. At the railway tracks, these authors estimated PGA's of 0.6 g or higher. Based on the review of several acceleration records, Carter and Seed (1988) considered an equivalent uniform harmonic acceleration record with peak acceleration equal to 50% of the actual PGA as a reasonable representation of the train accelerations. This approach was adopted in this study.

Train-induced ground vibrations consist predominantly of Rayleigh waves (Carter and Seed, 1988; Kim and Lee, 1998). Kim and Lee (1998) also found that significant amount of the energy went into shear (S) and compression (P) waves. A more detailed discussion regarding the types of waves generated by train traffic can be found in Carter and Seed (1988).

LIQUEFACTION OF RAILWAY EMBANKMENTS

Introduction

For the past 35 years, the area of soil liquefaction due to cyclic loading has been intensively studied. A number of different approaches have been proposed to calculate the liquefaction potential of soil deposits in true field conditions. Most liquefaction analysis procedures make the assumption that the sand deposit is under horizontal free-field ground conditions. Under such conditions, a soil element would have no initial or static shear stress on the horizontal plane, and would undergo fully reversed cycles of shear stresses when subjected to cyclic loading (Seed and Lee, 1966; Finn et al., 1971). However, there are many practical situations in which initial static shear stresses act on the horizontal plane of the soil element (e.g. dams, railway embankments, near buildings, etc). For these elements it is possible that no shear stress reversal occurs (during dynamic loading), depending mainly on the relative magnitude between the induced dynamic shear stresses and the initial static shear stress (Pando and Robertson, 1995). The response of cohesionless soils to cyclic loading is strongly influenced by the occurrence of shear stress reversal (Yoshimi and Oh-oka, 1975; Vaid and Finn, 1979). To include the influence of the initial static shear stresses (e.g. for sloping ground conditions) in the liquefaction design procedure, Seed and his co-workers suggested the use of a correction factor (K_α) (Lee and Seed, 1967; Seed, 1983; Seed et al. 1984; Seed and Harder, 1990). The use of the correction factor K_α is still commonly incorporated in modern liquefaction analyses (Harder and Boulanger, 1997). For this paper the liquefaction potential was assessed using the cyclic stress approach including the K_α correction factor. The following subsection outlines this approach.

Cyclic shear stress approach

The evaluation of the liquefaction potential of railway embankments subjected to train-induced vibrations can be carried out using the cyclic shear stress approach. In essence, the cyclic shear stress approach consists of comparing the cyclic shear stresses induced by the cyclic loading (usually expressed in terms of cyclic stress ratio, CSR) with the liquefaction resistance of the soil (expressed in terms of cyclic resistance ratio, CRR). The use of the cyclic shear stress approach allows for the inclusion of the effects of the initial shear stresses present in sloping ground situations.

The liquefaction resistance is commonly expressed in terms of the cyclic resistance ratio (CRR) defined as the ratio of the average cyclic stress (acting on the horizontal plane) that causes liquefaction and the initial vertical effective stress. The cyclic resistance ratio equation, as proposed by NCEER (1997), is as follows:

$$\mathrm{CRR} = (\mathrm{CRR})_1 \times K_\alpha \times K_\sigma \qquad (1)$$

Where:

CRR = the cyclic resistance ratio (τ_{av}/σ_{vo}') at the actual initial stress state (e.g. σ_{vo}', τ_s)

$(\mathrm{CRR})_1$ = the cyclic resistance ratio at the reference state (SPT correlation; $\sigma_{vo}' = 1$ tsf, $\tau_s=0$)

K_σ = correction factor for vertical confining stress, σ_{vo}'

K_α = correction factor for initial horizontal shear stress ($\alpha=\tau_s/\sigma_{vo}'$)

σ_{vo}' = initial vertical effective confining stress

τ_s = initial static shear stress acting on the horizontal plane.

Liquefaction potential for train-induced vibrations

To apply the above procedure to railway embankments, it was necessary to estimate representative values for train-induced cyclic stress ratios (CSR) and the cyclic resistance ratios (CRR). The procedure used to estimate these stress ratios is outlined in the following subsections.

Characterization of the train-induced loading (CSR) The dynamic shear stresses induced by train loading were estimated using dynamic analyses. The procedures of the dynamic analyses and their results are presented in the model section of this paper.

Characterization of the Liquefaction resistance (CRR) The cyclic resistance ratio is usually estimated based on either laboratory test or in situ tests. The liquefaction resistance will depend heavily on factors such as the initial state of the soil (density, confining stress, etc) and the nature of the dynamic loading.

As mentioned earlier an important difference between earthquake loading and train-induced vibrations is the significantly higher frequency content of train-induced vibrations. Hence, the number of representative load cycles that a soil element will undergo during train-induced vibrations is considerably larger than for earthquake vibrations (Szerdy, 1985). This is an important consideration since the level of cyclic shear stress required to liquefy a sand is heavily dependent on the number of loading cycles (Seed and Idriss, 1982; Szerdy, 1985). Carter and Seed's (1988) results showed typical ground motion for trains at about 5 seconds of strong shaking followed by about 20 seconds of lower intensity shaking. This translates into 100 to 200 cycles of equivalent average cyclic loading for train-induced vibrations with predominant frequencies between 20 to 40 Hz.

The liquefaction resistance, based on laboratory testing, is estimated from tests in which the samples are subjected to cyclic shear stresses of uniform amplitude at frequencies typically between 1 to 2 Hz. Based on laboratory tests one can obtain a curve relating the number of cycles (of uniform cyclic stress) required to cause liquefaction with the CRR. Figure 1 shows such a relationship based on data from Seed and Idriss (1982) and Szerdy (1985). This plot was originally proposed by Seed and Idriss (1982).

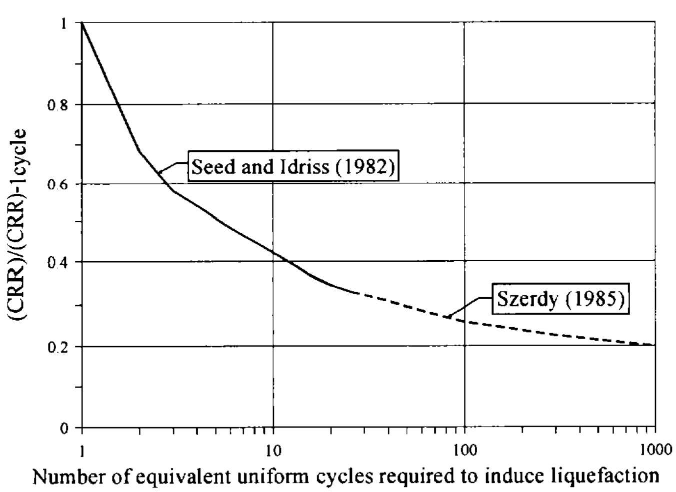

Fig. 1 – Influence of number of cycles required to cause liquefaction on lab based CRR

The liquefaction resistance for the problem of train-induced vibrations was estimated by modifying the SPT-based liquefaction resistance curve proposed by Robertson and Wride (1997). The SPT-based liquefaction resistance curve is appropriate for use in earthquake-induced liquefaction analysis when using the simplified procedure (Seed and Idriss, 1982) and specifically for a magnitude 7.5 earthquake. To estimate the applicable CRR for a loose, saturated sand subjected to train-induced vibrations one has to estimate a scaling factor to account for the difference in number of representative load cycles (Seed and Idriss, 1982, Carter and Seed, 1988). Using the relationship shown in Figure 1, the scaling factor can be estimated as the ratio of the CRR for 100 cycles (assumed representative for typical train loading) and the CRR for 15 cycles (assumed to characterize a magnitude 7.5 earthquake). The resulting scaling factor is about 0.68. This scaling factor was used to estimate the CRR curve for train-induced loading shown in Figure 2. This scaled CRR curve was used to estimate the liquefaction potential for the example problem presented in this paper. It should be noted that in a more detailed and rigorous analysis, CRR would be based on laboratory cyclic tests, ideally carried out at frequencies representative of the predominant frequency content of train-induced vibrations.

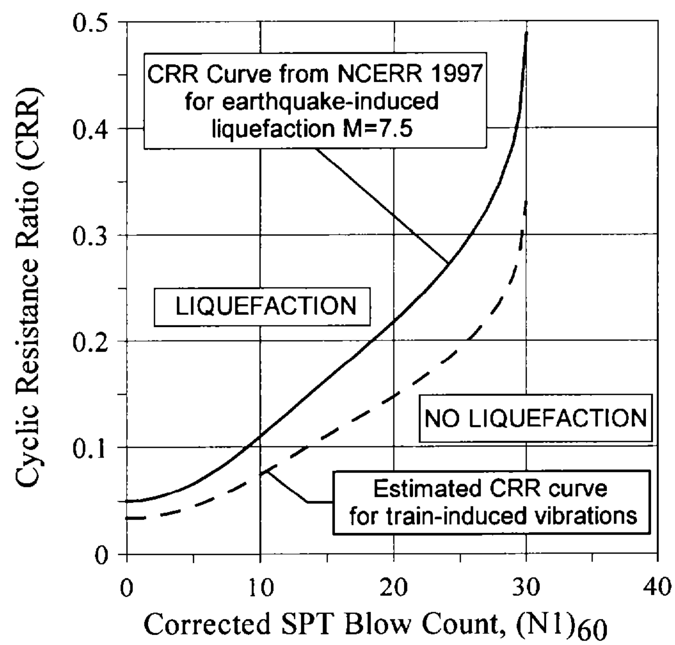

Fig. 2 – Estimated Cyclic resistance ratio for train induced vibrations

NUMERICAL MODEL – DESCRIPTION AND RESULTS

The computer program FLAC (Fast Lagrangian Analysis of Continua) was used for the numerical analyses carried out in this study. FLAC is a commercially available program (Itasca, 1998) that uses explicit finite difference scheme that can be used to solve a variety of two-dimensional static and dynamic problems.

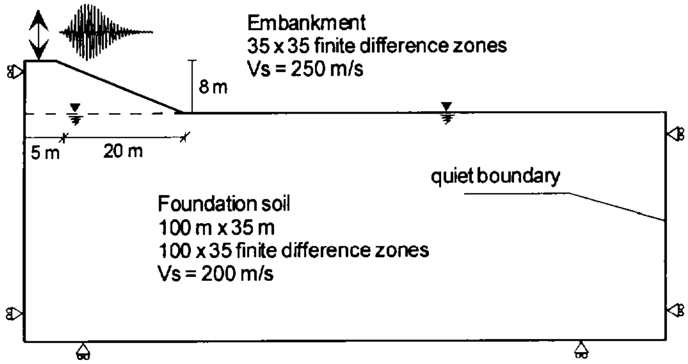

Fig. 3 – Geometry of the numerical model

This section summarizes the results of numerical analyses results carried out for a typical railway embankment under normal train loading. Figure 3 shows the railway embankment model used for the finite difference analyses. The model consists of two different zones. The embankment zone consists of a railway embankment 8 meters high with 2.5H:1V side slopes. The foundation zone is modeled as a loose-to-medium sand to allow is to assess the liquefaction potential of the embankment foundation. Ground water table assumed to be located at the elevation of ground surface.

The modeling was carried out using a linear elastic analysis, but the non-linearity was incorporated using an equivalent linear analysis with adjusted elastic properties to account for the expected level of shear straining. This was done using an iterative procedure.

Viscous damping was introduced to the vertical boundary away from the embankment using the quiet boundary scheme, built in FLAC, to prevent reflection of outgoing waves back into the medium. For the purpose of representing frictional energy losses, 5% damping is used for the entire model using Rayleigh type damping.

Displacements in the horizontal direction are constrained at the vertical boundary by the embankment to impose symmetry along the vertical axis. Finite difference grid zones were kept small enough to properly capture waveforms for the input frequency of 20 Hz, which is in the predominant range for train-induced vibrations (10 to 60 Hz). Waveforms associated with the input motion and waves expected to be generated within the medium (body waves and surface waves) can be captured with this model.

Numerical computations were done in two steps. First, a static analysis using a "switched on gravity" approach was carried out to estimate the initial static stresses. Figure 4 shows the horizontal shear stress contours obtained using this approach.

The second step involved the dynamic analysis. The train excitation was modeled as a harmonic excitation applied above the embankment at the approximate location expected for the railway tracks.

Vertical acceleration was applied at the top nodes of the embankment over a width of about 3 meters. The input time history was a synthetic sine wave acceleration time history with a frequency of 20 Hz and amplitude of 0.25g. The acceleration record was tapered with gradual increases and decays at the start and end of the record. Based on findings by Carter and Seed (1988), a peak ground acceleration of 0.25 g was selected to be representative of the average shaking induced by a train. In reality, the peak ground acceleration measured at the tracks is expected to be around 0.6 g or higher (Carter and Seed, 1988). The average level of shaking was selected to assess the liquefaction potential using the shear stress approach.

The shear stress ratio (α), defined as the ratio between the initial static shear stress (in the horizontal plane) and the vertical effective stress was also calculated. Figure 5 shows the contours of initial static shear stress ratio, α. These contours were used to determine the K_α correction factor discussed earlier in this paper. Values of K_α recommended for loose sands were used (Seed and Harder, 1990; Harder and Boulanger, 1997).

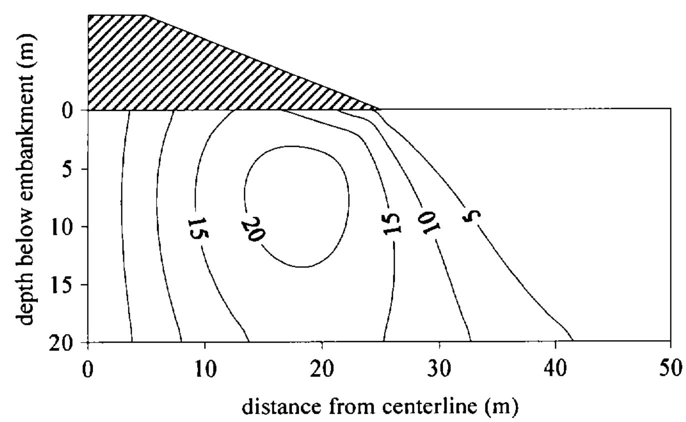

Fig. 4 – Static shear stress contours, $\tau_{xy\text{-}s}$ (kPa)

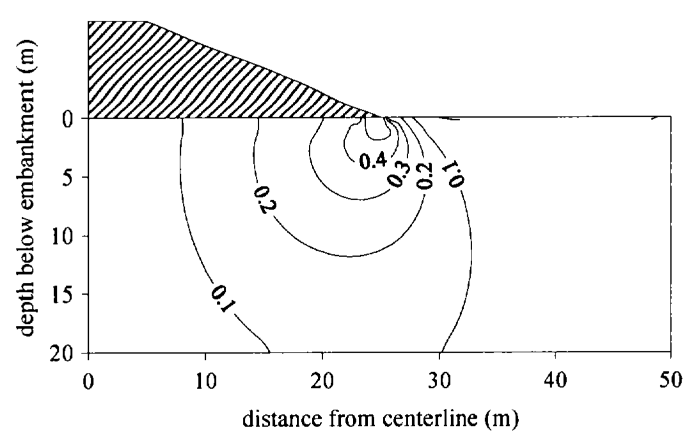

Fig. 5 – Static shear stress ratio contours - $\alpha = \tau_{xy\text{-}s}/\sigma_{vo}'$

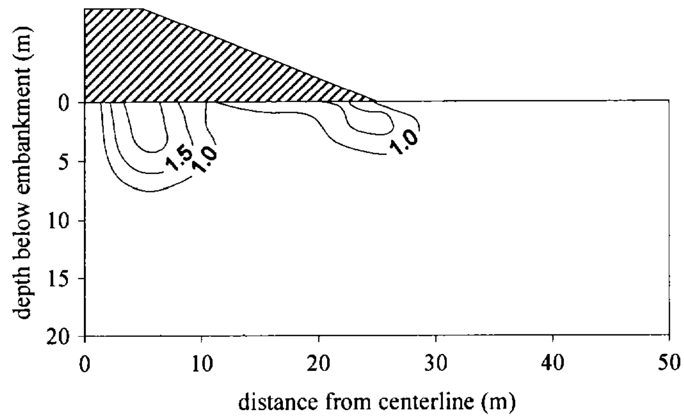

Fig. 6 – Contours of shear stresses on the horizontal plane induced by dynamic excitation, $\tau_{xy\text{-}dynamic}$ (kPa)

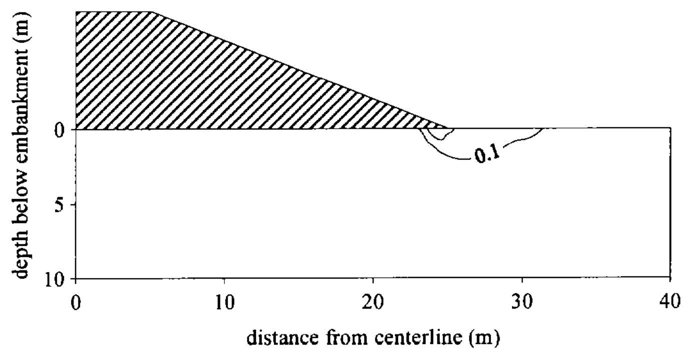

Fig. 7 – Cyclic stress ratio, $CSR = \tau_{xy\text{-}dynamic}/\sigma_{vo}'$

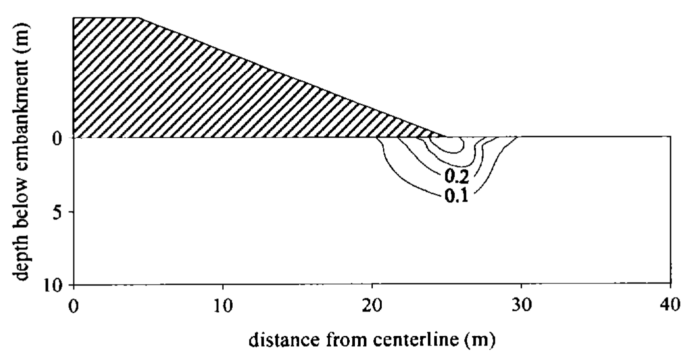

Fig. 8 – Contours of cyclic stress ratio (CSR) divided by K_α

Contours of dynamic shear stresses acting on the horizontal plane are shown in Figure 6. Contours of cyclic stress ratio within the railway embankment foundation are shown in Figure 7. Critical zones, where liquefaction potential is high, were detected based on normalized cyclic stress ratio contours obtained by dividing the CSR contours by the corresponding K_α factors (calculated based on the α contours). K_α was calculated using an average curve corresponding to a loose sand from the curves recommended by Harder and Boulanger (1997). Figure 8 shows the contours of normalized CSR. From this figure it can be seen that the critical zone, where liquefaction potential is high, is located towards the toe of the embankment extending to a depth of about 5 meters and over a length of about 10 meters.

Though not presented in this paper in detail, it has been observed from the results of the numerical analyses, that particle motion at and near the ground surface shows patterns similar to Rayleigh wave motion. The particle motion is predominantly elliptical with amplitude decreasing rapidly with depth.

The results presented in this paper are consistent with results presented by Carter and Seed (1988). Carter and Seed (1988) found that train-induced vibrations are capable of causing liquefaction of loose sand deposits with 10 degree slopes or steeper and to distances up to 45 feet from the tracks. More detailed studies are underway at Virginia Tech on this topic. These studies will incorporate numerical analyses involving non-linear material models and pore pressure generation models to further investigate dynamic behavior.

CONCLUSIONS

The liquefaction potential of railway embankments was evaluated following the shear stress approach and the K_α correction factor. The magnitude of shear stresses induced by train traffic was computed using the finite difference computer program FLAC. It was found that for a railway embankment 8 m high with 2.5H:1V side slopes, liquefaction can occur near the toe. The liquefaction potential was predicted to be high within an area 5 m deep and 10 m wide.

It was also found that the levels of normalized cyclic stress ratio (CSR/K_α) near the toe can be as high as 0.4. This may be critical for railway embankments with foundations soils composed of loose to medium dense sands with high water pressures due to a high water table or embankment seepage. In fact, many of the reported embankment failures have been associated with train-induced vibrations coupled with high pore pressure conditions. The presence of high pore pressures have a significant effect in minimum level of dynamic stresses required to induce liquefaction. The presence of initial static shear stresses (due to sloping ground conditions) was also found to have a significant effect on the liquefaction potential. For loose sands, the higher the initial shear stress ratio the lower the liquefaction resistance. This is in agreement with the field observations made in the majority of reported failures where train induced vibrations were found to be coupled with sudden rise of pore water pressures (e.g. due to poor drainage, flooding, heavy rainfall).

Further studies are necessary to investigate the dynamic behavior and liquefaction resistance. Parametric studies will help to understand the effects of slope geometry and nature of the input motion on estimated shear stresses.

ACKNOWLEDGEMENTS

Financial support for this study was provided by ECSUS (Earthquake Engineering Center for the Southeastern United States), newly established research center situated at Virginia Tech.

REFERENCES

Barneich, J. A. [1985]. "Vehicle induced ground motion.", Vibration Problems in Geotechnical Engrg., ASCE, October, pp. 187-202.

Carter, D. P. and H. B. Seed [1988] "Liquefaction potential of sand deposits under low levels of excitation." Report No. UCB/EERC-88-11, University of California, Berkeley, August, p. 309.

Griffin, M.J. and Stanworth, C.G. [1984] "The generation and perception of vibration from rail traffic' In Track Technology, U. Nottingham, U.K., pp. 215-223.

Harder, L. F. and R. Boulanger [1997] "Application of K and K correction factors.", Proceedings of the NCEER Workshop on Evaluation of Liquefaction Resistance of Soils, Technical Report NCEER-97-0022, December, pp. 167-190. Salt Lake City, Utah.

Hryciw, R. D., et al. [1990]. "Liquefaction and flow failure during seismic exploration.", Journal of the Geotechnical Engineering Division, ASCE, No. 116(12), pp. 1881-1899.

Itasca Consulting Group, Inc. [1998]. "FLAC – Fast Lagrangian Analysis of Continua User's Manual"

Kaynia, A. M., Madshus, C. and Zackrisson, P. [2000] "Ground vibration from high-speed trains: prediction and countermeasure" JGGE, ASCE, V. 126, No. 6, June, pp. 531-537.

Kim, D. S. and J. S. Lee [1998] "Source and attenuation characteristics of various ground vibrations.", Proc. Geotechnical Earthquake Engineering and Soil Dynamics III, GSP No. 75, ASCE, Seattle, WA, pp. 1507-1517.

Lee, K. and H. B. Seed [1967] "Dynamic strength of anisotropically consolidated sand.", JSMFE, ASCE, No. 93(5), pp. 169-190.

Madshus, C., A. M. Kaynia, L. Haruik, and J. K. Holme [1999] "*A numerical ground model for railway-induced vibration.*" Norwegian Geotechnical Institute Publication No. 205, pp. 45-55.

NCEER. [1997]. "Summary report." Proc. NCEER Workshop on Evaluation of Liquefaction Resistance of Soils, Report NCEER-97-0022, December, pp. 1-40. Salt Lake City, Utah.

Pando, M. A. and P. K. Robertson [1995] "Evaluation of shear stress reversal due to earthquake loading for sloping ground", Proc. 48th Canadian Geotechnical Conference, Vancouver, BC, Vol. II, pp. 955-962.

Robertson, P. K. [1994]. "Suggested terminology for liquefaction", Proc. 47th Canadian Geotechnical Conference, Halifax, NS, pp. 277-286.

Seed, H. B. [1983]. "Earthquake-resistant design of earth dams", Proc. Symposium on Seismic Design of Embankments and Caverns, ASCE, Philadelphia, PA, pp. 41-64.

Seed, R. B. and Harder, L. F. Jr. [1990] "SPT-based analysis of cyclic pore pressure generation and undrained residual strength", Proc. H. Bolton Seed Memorial Symposium, pp. 351-376.

Seed, R. B. and Idriss, I. M. [1982] "Ground motions and Soil Liquefaction during earthquakes" EERI Monograph.

Szerdy, F. S. [1985]. "Flow slide failures associated with low level vibrations." Ph.D. Dissertation, Dept. of Civil Engineering, University of California, Berkeley, 282 p.

Vaid, Y. P. and J. C. Chern [1983] "Effect of static shear on resistance to liquefaction." Soils and Foundations, JSSMFE, No. 23(1), pp. 47-60.

Vaid, Y. P. and W. D. L. Finn [1979] "Static shear and liquefaction potential." ASCE Journal of the Geotechnical Division, No. 105(10).

Zackrisson, P. [1997]. "Effects of passing trains on the stability of railroad embankment foundations", Proc. Of the 14th International Conference of Soil Mechanics and Foundation Engineering, Vol. II, Hamburg, Germany, pp. 1057-1062.